Composites Part A 115 (2018) 134–146

Contents lists available at ScienceDirect

Composites Part A

journal homepage: www.elsevier.com/locate/compositesa

Experimental investigation on spring-back deformation during autoclave curing of parabolic antenna reflectors

Dhaval B. Shah[a], K.M. Patel[a], Arvind I. Patel[b], Vishwajit Pariyal[b], Shashikant J. Joshi[a,*]

[a] Mechanical Engineering Department, Institute of Technology, Nirma University, S-G Highway, Ahmedabad, India
[b] Senior Scientist – Engineer, Antenna Division, Space Applications Center, Indian Space Research Organisation (ISRO), Ahmedabad, India

ARTICLE INFO

Keywords:
A. Polymer-matrix composites
E. Prepreg
E. Autoclave curing
Spring-back deformation

ABSTRACT

High dimensional fidelity is the primary challenge for the large size carbon fiber reinforced polymer (CFRP) antenna reflectors used in space applications. Selection of crucial process parameters governs dimensional control of a composite product. In this paper, the influence of the mould materials, curing cycle, lay-up sequence and laminate thickness on spring-back deformation during autoclave curing is investigated by fabricating a large number of parabolic reflectors using the unidirectional prepreg system. The non-contact type accurate 3D scanning technique is used to measure the dimensions of the parabolic antenna reflectors. In the present work, an experimental approach is adopted for the determination of a combination of process parameters which gives minimum spring-back deformation. The results reveal that the spring-back deformation of parabolic reflectors is significantly affected by the mould material and laminate thickness, whereas the lay-up sequence and curing cycle do not have a significant effect.

1. Introduction

Last few decades have witnessed a considerable increase in the use of CFRP mainly for aerospace structures, marine components and sporting goods. Prepegs are thin sheets containing fibers and uncured resin [1]. Use of prepregs for composite manufacturing offers the advantage of high fiber volume fractions and an adaptability for manufacturing complex parts. Autoclave curing is widely practiced because of its robustness and has attracted the attention of industries and researchers [2]. As autoclave curing is preferred for complicated parts requiring good dimension stability, warpage, spring-back deformation and process induced deformations must be minimal. The parabolic shape antenna reflectors used in the space communication satellites are made from CFRP. It is very much essential that the profile of CFRP reflector should confirm that of mould and a small deviation will result in an improper functionality of the reflector. A large number of experimental investigations have been conducted to minimise the deviation of the antenna reflectors. Many researchers have studied the effect of various parameters on the spring-back for flat and angled components and findings are summarized in the following paragraphs.

The two prominent defects in angled composite laminates are spring-back and warpage. Warpage denotes the initially plane surface becoming curved whereas spring-back or spring-in denotes a change in the enclosed angle between two planes. The development of residual stresses in the part and the mould is inevitable during manufacturing of composite laminates as, the parts cure at high temperatures. Hahn and Pageno [3] divided their study in two parts. Firstly, the total strain in the laminate was decomposed as consisting of thermal strain and mechanical strain. Secondly, considering resin matrix properties, curing stress was determined based on the thermal strain. Beginning with an assumption that the temperature is constant along the thickness of the thin laminate, a mathematical model to predict the residual strains and cure kinetics was developed by White and Hahn [4]. It was noted by Twigg et al. [5] that debonding, sliding of the part starts at the end and progresses towards the centre. Further, they carried an experimental investigation of warpage due to a tool part interaction resulting in the development of an empirical relationship for warpage by considering pressure, part length and part thickness as process parameters. They developed a numerical model using finite element software for shear stress along the tool part interface [6]. Kaushik and Raghvan [7] measured static and dynamic friction coefficients during the autoclave curing. Oliveira et al. [8] studied an influence of mould material and lay-up sequence on warpage experimentally. The strain in composite laminate was measured using embedded optical fiber bragg gratings. The effect of part thickness, type of prepreg, part length, curing cycle, a material of mould and surface roughness of mould on the warpage for flat composites was considered by Stefaniak et al. [9]. Experiments conducted by Albert and Fernlund [10] explored the effect of flange

* Corresponding author.
E-mail address: s.j.joshi@nirmauni.ac.in (S.J. Joshi).

https://doi.org/10.1016/j.compositesa.2018.09.017
Received 19 April 2018; Received in revised form 6 September 2018; Accepted 20 September 2018
Available online 22 September 2018
1359-835X/

length, tool material, curing cycle, lay-up sequence, part angle and part thickness on spring-in and warpage.

Most of the analytical models proposed by various researchers were based on closed-form solutions and the classical lamination theory [11–15]. In their early work, Nelson and Cairns [16] proposed an analytical equation for spring-in based on the classical lamination theory so that effect of thermal strain, chemical shrinkage and the residual strain was included. Bapanapalli and Smith [17] described that spring-in depends on many parameters like cure temperature, applied pressure, part geometry, part material, part thickness, lay-up sequence, mould surface and mould thermal expansion. A numerical linear elastic model was developed which describes mould stretching, thickness shrinkage and volume fraction gradient independently. Darrow and Smith [18] concluded that for thin parts (< 2 mm) spring-in was dominated by fiber volume fraction gradient and mould stretching effects whereas for thick (> 2 mm) parts spring-in was dominated by thickness cure shrinkage. Kappel et al. [19] established semi-analytical simulation strategy as well as executed experiments for flat components to predict warpage with part length and part thickness as parameters. Kappel et al. [20] performed an experimental study on the L-shaped samples by considering lay-up sequence, part thickness, part radius and mould material as parameters to predict process induced distortion. The semi-numerical methodology was established to predict manufacturing distortions of a CFRP box-structure [21].

It is evident from the literature that very few studies were devoted to the spring-back of curved CFRP composites. Wisnom et al. [22] developed an analytical model for spring-in due to chemical shrinkage occurring and identified that vitrification and thermal strains were responsible for this kind of behaviour. The model was however very simple as it ignores interaction of tool and part because of difference in coefficient of thermal expansion. Another analytical model of Vargas et al. [14] deals with a development of Airy's strain function for curved composite laminates treating them as beams. Kappel [23] conducted experiments on curved shape CFRP panels to predict process induced distortion and validated previous analytical models. Although a lot of work has been reported for spring-in and warpage during an autoclave curing of flat and angled composite laminates, experimental studies related to curved composites have been rarely reported in the literature. The antenna reflector is a standalone device used for redirecting radio frequency energy or reflects electromagnetic waves in satellite communications. The antenna reflector is a portion of a circular paraboloid, generally obtained by intersecting a parabolic surface with a cylinder [24]. These high precision parabolic shape reflectors are made from CFRP material using an autoclave manufacturing process with backup structure [25]. The prime objective of this work is to investigate the effect of various process parameters viz. mould material, part thickness, lay-up sequence and curing cycle on spring-back deformation of the parabolic antenna reflectors during an autoclave curing.

2. Experimental details

The size of an antenna reflector used in the space applications is varying in the range of 0.8 m to 12 m diameters as per gain requirement. To study the effect of various process parameters on dimensional accuracy and to conduct experimentation, prototype CFRP antenna reflectors of 240 mm are manufactured in the present work. The size of a reflector is calculated based on the tenth scale of one of the actual size for antenna reflector i.e. 2.4 m. The focal length and depth of parabola are calculated based on the diameter and feed to depth ratio of the reflector. The ratio of prototype model to actual model dimensions is kept same for each parameter.

The following steps have been identified to fabricate the parabolic antenna reflectors and subsequent measurement of its spring-back deformation.

- The preparation of 3D CAD model of a parabolic reflector mould and its subsequent fabrication.
- Layups of prepreg layers along with consolidation materials.
- Curing in an autoclave machine succeeded by demoulding of the reflector.
- Measurement of dimensions of the fabricated reflectors.
- Comparison of coordinates of the fabricated reflectors with the theoretical CAD model and consequent determination of spring-back deformation.

2.1. Experimental procedure

The 3D CAD model of a parabolic reflector and a corresponding mould have been prepared based on the calculated dimensions using a solid modelling software. The parabolic surface has been generated by rotating a curve, which has been created from an equation of a parabola. Initially, parabolic shape moulds have been prepared using various mould materials namely grey cast iron, stainless steel, graphite and invar. The blocks of different mould materials having size 300 × 300 × 70 mm have been procured. The criteria for selecting the mould materials have been described in Section 2.2 in detail. The 5-axis vertical machining centre (VMC) has been used to manufacture the parabolic moulds and a special part program has been developed for the same. An identical surface finish has been achieved for each mould during the machining.

The moulds have been cleaned and degreased with acetone to remove residues of handling, previous curing cycles as well as run-to-run variability before using them. Three coats of Loctite Frekote 55-NC release agent have been then applied over the entire surface with a 15 min drying interval between two consecutive coats. Preliminary tests using the actual prepreg system have been performed to estimate the influence of unavoidable run-to-run changes within identical experimental setups before carrying out the main experiments.

To prepare the parabolic reflectors, the number of layers of the cut prepreg has been placed on the cleaned surface of the mould. The selection of prepreg system and consolidation materials have been discussed in Section 2.3. After each layer of carbon fiber lamina prepreg, normal hand pressure has been applied to remove the entrapped air between two consecutive layers of prepreg. One layer of peel ply and two layers of breather cloth with the same size have been placed on the top of the prepreg layers (Fig. 1). Thermocouples have been placed on the parts, near the mould and the bag surfaces. The entire setup has been vacuum bagged using vacuum film, sealant tape and Airtech made vacuum valve along with a hose pipe. Subsequently, the vacuum has been applied for at least thirty minutes to achieve proper consolidation and to remove air residues. The line diagram of an entire setup is shown in Fig. 1. After the bagging is finalized, the whole setup has been placed into an autoclave machine as shown in Fig. 2. All components have been cured as per designed curing cycle in a laboratory scale autoclave machine, which is having working space of Φ 900 mm × 1 m length.

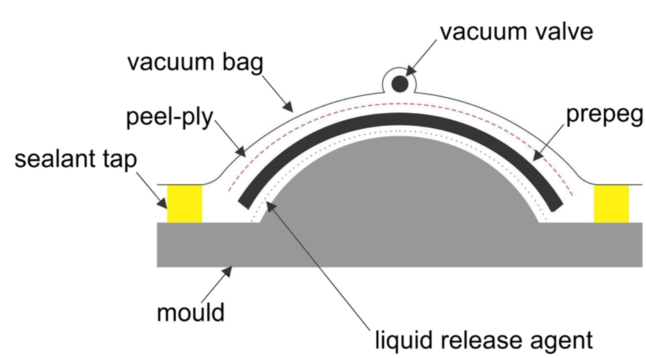

Fig. 1. Line diagram of consolidation materials along with mould. (For interpretation of the references to colour in this figure legend, the reader is referred to the web version of this article.)

Fig. 2. Parabolic antenna reflectors cured in an autoclave machine.

The detail of the curing cycles has been given in detail in Section 2.4. Initially only one component has been cured, later on, three components have been cured simultaneously with same curing cycle with different mould materials in an autoclave machine as shown in Fig. 2 to reduce total experimentation time.

The manufactured reflectors have been kept in open atmospheric temperature for almost twenty hours after taking out from an autoclave machine for post curing to reduce the residual stresses. The consolidation materials, as well as a composite reflector, have been demoulded from the mould sequentially. The demoulded cured reflector is shown in Fig. 3, ready for spring-back measurement using 3D scanning. Some of the reflectors have been manufactured again which are failed during the autoclave curing process because of the insufficient vacuum, delamination or break down of laminate while demoulding. The same procedure has been repeated to manufacture all the parabolic reflectors used for the experimental work.

2.2. Selection of mould materials

Mould and composite part interaction, hence coefficient of thermal expansion (CTE) of the mould material is an important factor affecting the generation of residual stresses as well as spring-back deformation during the curing process. The mould material which is having similar CTE value as a composite product gives a lesser amount of post cure deformation. The availability of the material in various sizes, machining time, surface finish, special tooling and process required for machining, etc. have also been considered while selecting the mould materials. Grey cast iron grade 30, stainless steel AISI 430, EDM grade graphite and invar 36 have been selected as mould materials for manufacturing the reflectors. The mechanical properties of these materials are listed in Table 1.

Grey cast iron grade 30 (ISO 200) is normally used as a mould material for the manufacturing of satellite communication reflectors due to its ease of availability and manufacturability [26]. The parabolic shape cast iron mould has been prepared via sand casting process using a wooden pattern. Stainless steel is considered as an alternate mould material due to ease of availability, cost-effectiveness and its good machinability. AISI grade 430 is selected because of its low CTE when compared with various grades of stainless steel like AISI 202, 304, 316, 310, 410. However, the cost of raw material and machining is higher when AISI grade 430 is compared with cast iron.

Fig. 3. Cured antenna reflector.

Graphite and invar are very good candidates as alternative mould materials due to the proximity of their CTEs with that of CFRP. The problem with graphite material is non-availability in a large size as well as an environmental hazard while its machining. The particle formation during graphite machining may damage the functionality of a machine tool as well as degrade the quality of coolants. The EDM grade graphite is recognised as a good candidate mould material because of its lower CTE as well as lower grain size when it is compared with other grades of graphite like GLM, FE679, IC-6002, and IC-6003. The mirror grade surface finish on the top surface of a graphite mould is achieved by machining followed by a lapping process. The additional care is taken while handling a finished graphite mould during transportation due to its fragile nature. Being a non-economical and difficult to machine poses the limitations on the use of invar as a mould material. The invar 36 grade is selected for making the mould because of its lower CTE. The diamond cutting tools are used for machining of invar by selecting a proper machining speed to achieve a good surface finish. The cost of raw material and machining are higher in the case of invar in comparison to other alternate mould materials. The machined moulds of cast iron, stainless steel, graphite and invar materials with almost identical surface finish are shown in Fig. 4.

2.3. Caron fiber prepreg system and consolidation materials

The prepreg material HCU200/A45, carbon/epoxy unidirectional tape manufactured by Hindoostan Technical Fabrics Company is used in this study for the manufacturing of parabolic reflectors. It is non-bleed toughened prepreg with a cure temperature of 160 °C. The prepreg material HCU200/A45 contains HCU200 unidirectional fibers pre-impregnated with A45 toughened epoxy resin. The resin has an elastic modulus of 2.915 GPa and a tensile strength of 48 MPa, formulated for the autoclave curing process [27]. The HCU200 consists of continuous carbon fibers tows with a filament diameter of about 7 µm and a moderate elastic modulus of 230 GPa. These fibers are manufactured using 12 K tows with areal weights 200 g/m^2. The prepreg system has been stored at −18 °C in a sealed condition with a shelf life of twelve

Table 1
Mechanical properties for selected mould materials.

Mould materials	Coefficient of thermal expansion (CTE) (µm/m/°C)	Thermal conductivity (W/m K)	Specific gravity (gm/cm^3)
Cast iron grade 30 (ISO 200)	10.5	46	7.2
Stainless steel AISI 430	11.2	25	7.8
Graphite EDM	4.4	139	1.86
Invar 36	1.6	13	8.1

months from the date of manufacture.

The release agent, peel ply, breather fabric, vacuum bag and sealant tape are used for the consolidation of an antenna reflector during an autoclave process. The grades for these materials are identified such that they are compatible with planned autoclave curing. The release agent prevents the adhesion of composite lay-up with the mould during curing process as well as decreases the coefficient of friction between the mould and the part. The peel ply allows free passage of volatiles and excess matrix during the cure. The breather fabric applies a uniform vacuum pressure and also helps in removal of air and volatile from entire assembly. The vacuum bag and sealant tape seals the entire assembly and provide passage for the removal of air and volatiles.

2.4. Curing cycles

The curing cycle is a representation of the combination of pressure and temperature which are applied to the vacuum bagged assembly during the autoclave processing. The single hold (SH) curing cycle has been designed so that gelation of the resin occurs during the temperature hold whereas the double hold (DH) cycle has been designed to achieve gelation prior to the second heat-up which are compatible with the prepreg manufacturer's recommendation. The point of gelation has been estimated based on calculations using cure kinetics equations for the prepreg system [10]. The single hold cycle consists of a ramp up of 2 °C/min up to 160 °C with holding time 120 min and ramp down of 2 °C/min. The double hold cycle consists of first ramp up of 2 °C/min up to 110 °C, a first hold at 120 °C for 60 min, a second ramp up of 2 °C/min up to 160 °C, a second hold at 160 °C for 120 min and ramp down of 2 °C/min. The pressure of 5 bar is applied throughout the curing cycles as shown in Fig. 5. During a single hold and double hold curing cycles, the temperature of laminate, pressure of an autoclave chamber and vacuum pressure have been recorded at every minute in an autoclave machine (Fig. 6(a) and (b)). The actual reading of the temperature of the laminate is slightly lagging compared to a set temperature.

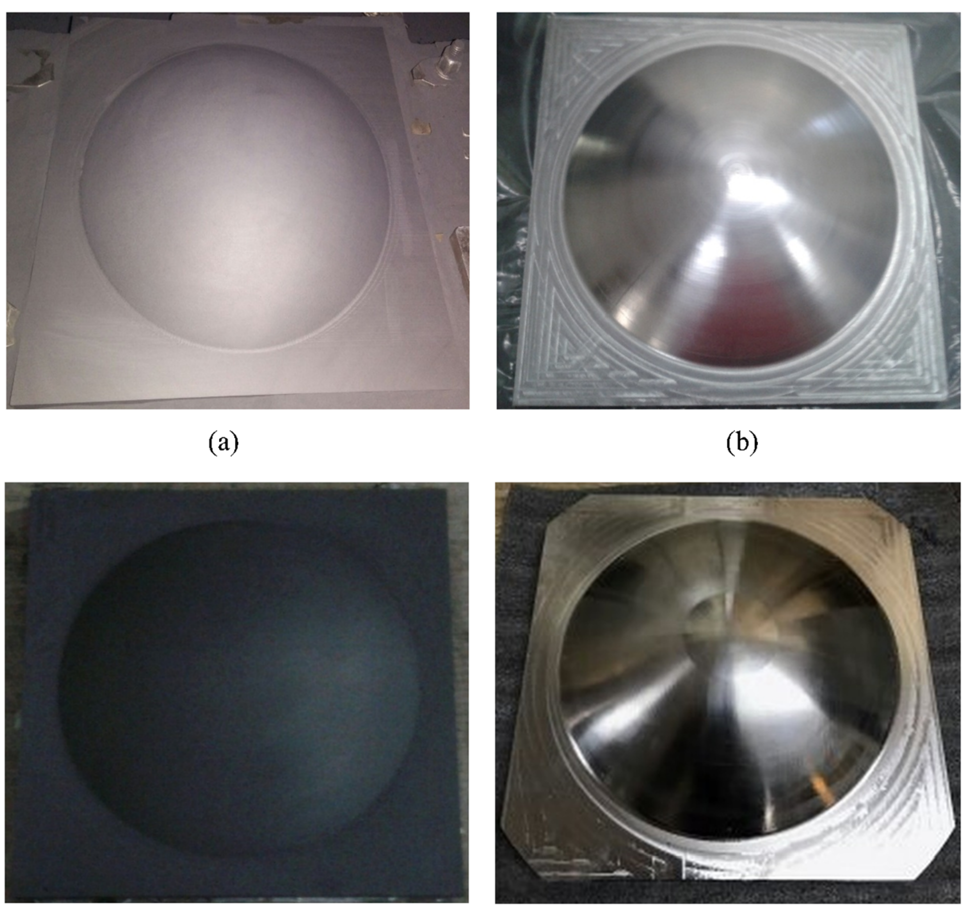

(a) (b) (c) (d)

Fig. 4. Machined moulds (a) Grey cast iron grade 30 (b) stainless steel AISI 430 (c) graphite EDM (d) Invar 36.

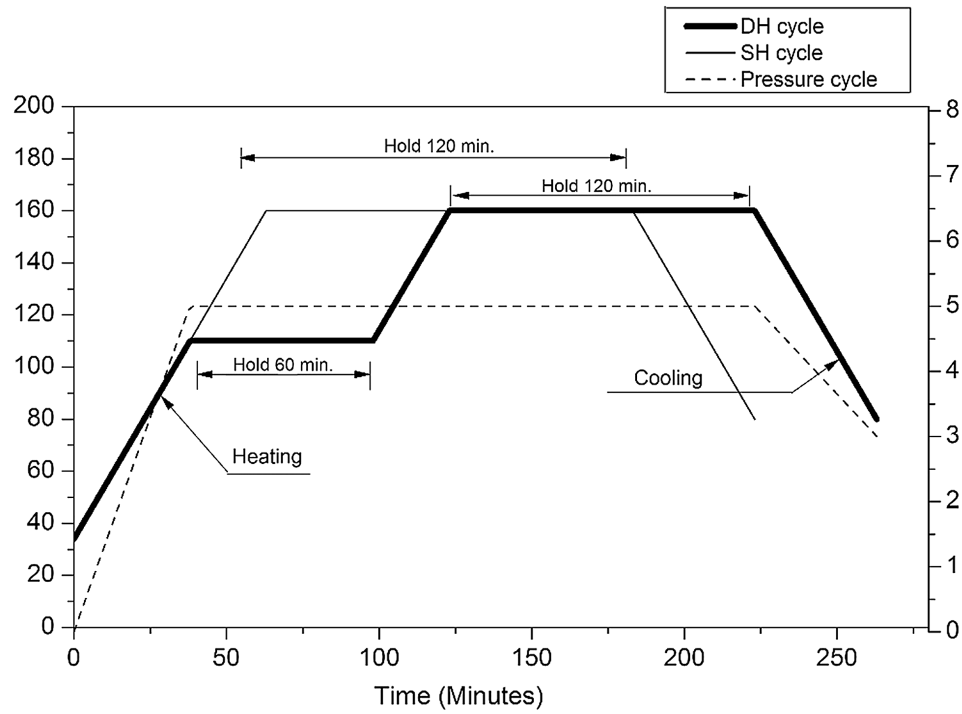

Fig. 5. Theoretical single hold and double hold curing cycle applied to an autoclave machine.

2.5. Parametric details

The present experimental study focuses on four process parameters namely mould materials, lay-up arrangements, the thickness of laminates and curing cycle and their effect on spring-back deformation. As shown in Fig. 7, four types of mould materials, three types of lay-up sequences, three types of laminate thicknesses or number of layers and two types of curing cycles have been considered. Total seventy-two reflectors are manufactured as per full factorial design using an autoclave curing process. The mould materials considered and curing cycle selection have already been discussed in previous Sections 2.2 and 2.4 respectively. The standard lay-up sequences i.e. uni-directional, cross and quasi-isotropic lay-up have been considered as suggested by multiple authors [1,8,10,15,20,28,29]. The unusual and unsymmetric lay-up sequences have not been considered because of the risk of delamination and premature failure [30]. The laminate thickness has been restricted up to 2 mm as per the requirement of space communication antenna [26]. The prepreg material, an autoclave pressure, bagging arrangement and the release agent used are identical throughout the study in order to preclude affectations due to these parameters. The pressure applied while laying prepreg on the mould is assumed to be constant. All reflectors in this study have been fabricated using single bagging arrangement in order to blank out the effects of the bagging. Thus, it can be concluded that the spring-back deformation is the function of mould material, curing cycle, lay-up sequence and laminate thickness. Confirming experiments have been performed to ensure the observed trend, repeatability as well as consistency between batches.

3. Measurement of spring-back deformation of the reflectors

Looking to the requirement of a gain and an efficiency of the space communication antennas, diameter $D = 240$ mm and $f/D = 0.33$ have been considered to study the spring-back deformation [26,31]. The focal length f mm and depth c of the parabolic reflector have been calculated using Eq. (1) and same are 80 mm and 45 mm respectively.

$$f = \frac{D^2}{16c} \tag{1}$$

The 3D CAD solid modes for the reflector and corresponding mould have been prepared using these dimensions. Total 200 coordinate points have been obtained by generating circles of diameters 50, 100, 150, 200 and 240 mm at the inner surface of the parabolic reflectors. These coordinate points have been identified at an outer parabolic surface of the mould as well as an inner surface of the reflector with centre top point as a reference point. The 40 points on the circumference of each circle have been obtained at every 9° angular position (Fig. 8a).

A high precision 3D scanning technique has been used for the measurement of specified coordinates on the mould sided surface of the reflectors. The optical measurement system is able to capture the coordinate positions without touching the reflectors to eliminate adulterating effect due to the hand or the tool forces as in the case of coordinate measuring machine (CMM). The Freescan X5 high speed 3D scanner with measuring accuracy of 25 µm has been used for the scanning at an internal surface of the manufactured reflectors. The developer spray has been applied on the surface of the reflector to highlight the black surface. The scanned surface has been generated based on the marked reference points using scanning software. The point cloud data has been generated using a commercially available software geometric design X, which is compatible with 3D scanner (Fig. 8b). This generated surface has been superimposed with original CAD surface to find the deviation of the predefined coordinate points. The deviation between every coordinates points of CAD model and manufactured reflectors have been determined using scanning software (Eq. (2)).

$$\text{Deviation } d_n = \sqrt{(x_{an}-x_{tn})^2 + (y_{an}-y_{tn})^2 + (z_{an}-z_{tn})^2}, \quad n = 1, 2, \cdots 201. \tag{2}$$

where, x_a, y_a, z_a are actual x, y and z coordinates measured using 3D scanner while x_t, y_t, z_t are theoretical x, y and z coordinates obtained from 3D CAD model. The deviation at each point is given as d.

The root means square (RMS) of all the deviations has been calculated using Eq. (3), which referred as the spring-back deformation for the corresponding reflector.

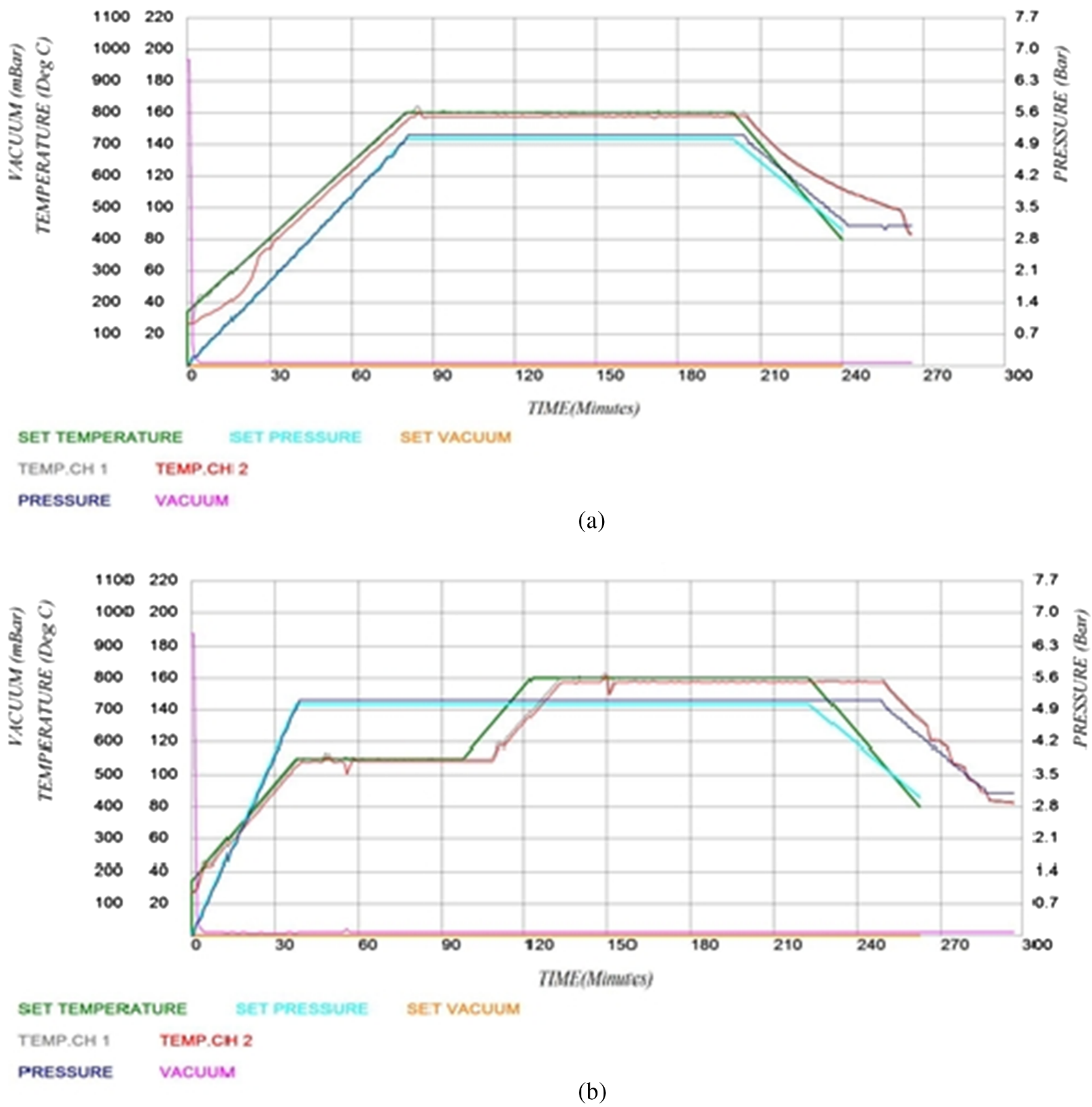

Fig. 6. Actual (a) single hold (b) double hold curing cycle recorded during the autoclave process. (For interpretation of the references to colour in this figure legend, the reader is referred to the web version of this article.)

$$S_{rms} = d_{rms} = \sqrt{\frac{1}{n}(d_1^2 + d_2^2 + \cdots + d_n^2)},\ n = 201 \tag{3}$$

Here, S_{rms} is the spring-back deformation of the reflector.

The similar procedure has been adopted for each manufactured reflector. To assess the uncertainty of the measurement, the procedure of the measurement has been repeated thrice. This set of measurements reveals a standard deviation of ± 0.02% accuracy.

4. Results and discussion

The effect of the various process parameters, mould materials, curing cycle, lay-up sequence and laminate thickness on the spring-back deformation is discussed in the subsequent subsections. Full factorial design based on Taguchi approach is selected to understand main as well as the effects of interactions on the spring-back deformation.

4.1. Effect of mould materials

The mould material plays a major role in the components' shape distortion compared to other process parameters. The mould-part interaction due to the difference in the coefficient of thermal expansion of a mould and a composite part has a significant effect on the final deformation of an antenna reflector. In this study, it is made sure that all the moulds used for the reflector fabrication have an almost similar surface finish. Total 18 experiments have been conducted considering other process parameters namely curing cycle, lay-up sequence and laminate thickness same for each mould materials. It is clearly seen from Fig. 9 that the median RMS value of the spring-back deformation of the reflectors using an invar ($\alpha = 1.6\,\mu m/m/^{\circ}C$) mould is least compared to other mould materials – cast iron, stainless steel and graphite. This is because of less difference in CTE of invar and composite CFRP material. The median value of the spring-back deformation for the reflectors fabricated using a graphite ($\alpha = 4.4\,\mu m/m/^{\circ}C$) mould is more than the reflectors fabricated using an invar mould followed by cast iron ($\alpha = 10.5\,\mu m/m/^{\circ}C$) and stainless steel ($\alpha = 11.2\,\mu m/m/^{\circ}C$) moulds. The difference in the minimum spring-back deformation of the reflectors fabricated using the graphite and invar mould is 0.025 mm, whereas the difference in median spring-back deformation between them is 0.01 mm. The difference in minimum spring-back deformation

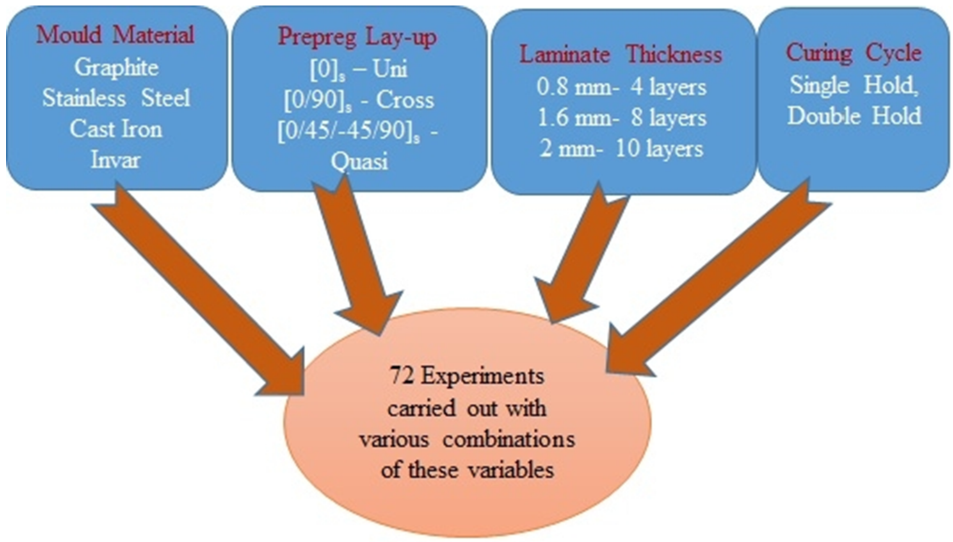

Fig. 7. Process parameters considered during experimentation for the reflectors manufacturing. (For interpretation of the references to colour in this figure legend, the reader is referred to the web version of this article.)

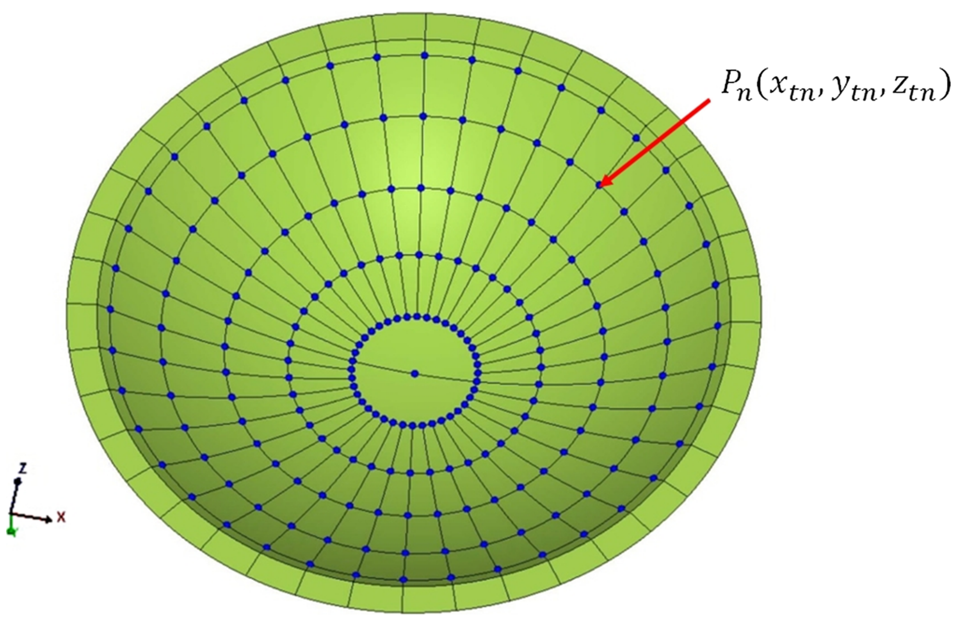

Fig. 8a. Theoretical x_t, y_t, z_t coordinates obtained from the 3D CAD model of the reflector. (For interpretation of the references to colour in this figure legend, the reader is referred to the web version of this article.)

for stainless steel and cast iron is 0.025 mm, whereas the difference in median spring-back deformation between them is 0.03 mm. The results of the experimentation suggest that the CTE is the significant parameter affecting the spring-back deformation observed in the reflectors. The measurement median bars in Fig. 9 indicate the experimental dispersion of maximum and minimum RMS values.

4.2. Effect of curing cycles

The effect of a single and double hold curing cycles on the spring-back deformation of an antenna reflector is studied by combining other process parameters like mould materials, lay-up sequence and laminate thickness. Fig. 10 shows the median value of the spring-back deformation occurred in the reflectors is minimum in the case of a single hold curing cycle compared to a double hold curing cycle. These results are in good agreement with results obtained by Fernlund et al. [28,32]; but are in disagreement with results obtained by White and Hahn [4]. The premise is that the resin gels on hold at 160 °C for a single hold curing cycle whereas it gels on the first hold at 110 °C for the double hold curing cycle. An extra spring-back deformation induced in the part is due to induced stresses produced during the double hold curing cycle. The induced stresses are the result of a high thermal expansion of the mould during the second heat up at 160 °C. During the experimentation, a release agent is used on the mould surface and due to that, the mould can stretch the part because of geometrical locking of the part on the mould.

4.3. Effect of lay-up sequences

The unidirectional $[0]_s$, cross $[0/90]_s$ and quasi-isotropic $[0/45/90/-45]_s$ are considered as lay-up sequences. Total 24 experiments, six for each mould material have been conducted with different curing cycles and laminate thicknesses for each lay-up sequences. It is clear from Fig. 11 that, quasi-isotropic lay-ups have minimum spring-back

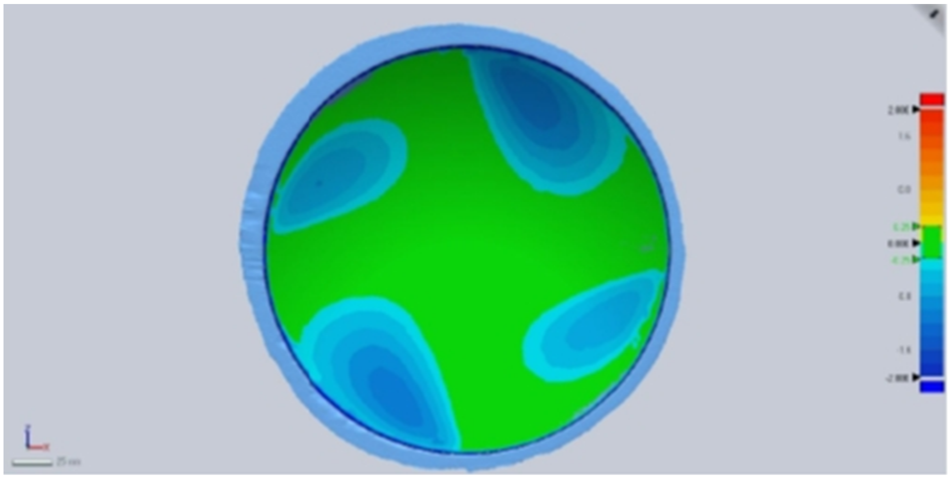

Fig. 8b. The contour plots of actual coordinates (x_a, y_a, z_a) obtained through 3D scanning. (For interpretation of the references to colour in this figure legend, the reader is referred to the web version of this article.)

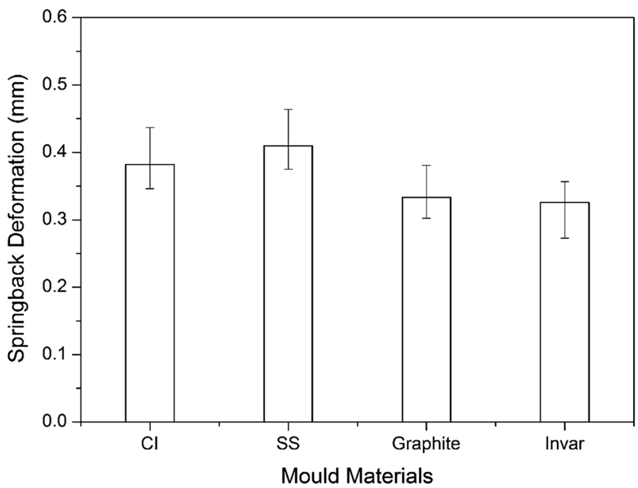

Fig. 9. Effect of mould material on spring-back deformation.

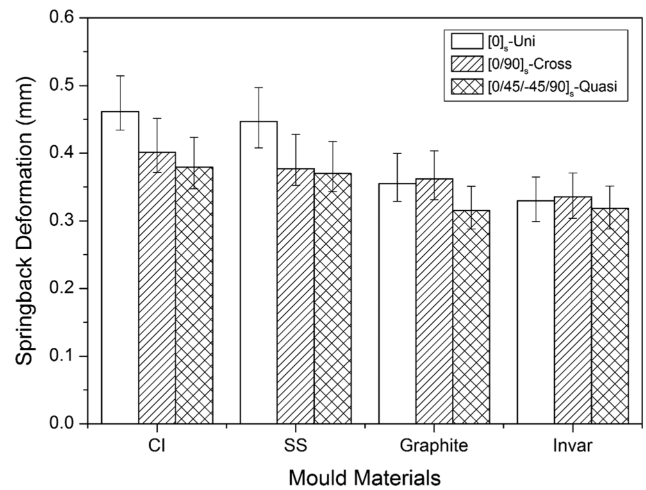

Fig. 11. Effect of lay-up sequence on spring-back deformation.

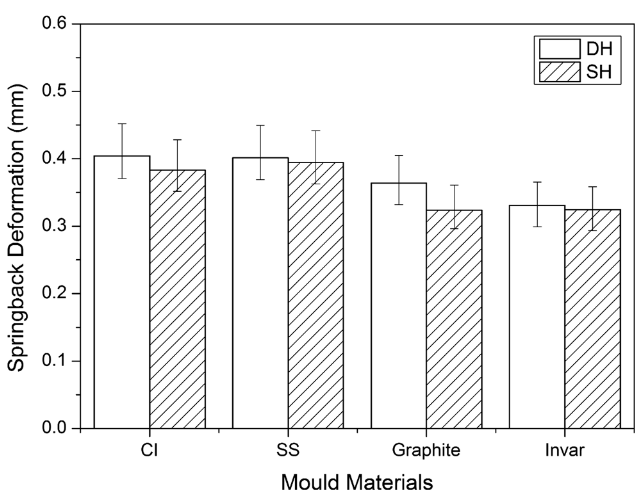

Fig. 10. Effect of curing cycle on spring-back deformation.

deformation compared to unidirectional and cross lay-ups. It has been observed that lay-up sequence does not have a significant effect on the spring-back deformation because lamina orientation affects the warpage, but do not affect spring-back deformation significantly. This observation is in the good agreement with results obtained by Fernlund et al. [11] and Jain et al. [33]. It may be occurred because of through-thickness contraction due to Poisson's effect during anisotropy calculations. The other reason for more spring-back deformation in the case of cross laminates is the difference between the in-plane and through thickness thermal expansion coefficients. The greater spring-back deformation of unidirectional laminates as compared to quasi-isotropic laminates is because of thin laminates which suppress both large out-of-plane thermal strains of unidirectional laminates and the much smaller strains of quasi-isotropic laminates in this direction. The quasi-isotropic laminate has equal bending stiffness in all in-plane direction [29]. In the case of unidirectional lay-ups, modulus and thermal expansion of each ply are identical. During cool-down and demoulding stage, the internal strain is increased due to the large difference in the effective coefficients of thermal expansion between mould materials and composite part. So, the spring-back deformation of unidirectional is larger than cross-ply for the case of cast iron and stainless steel moulds. The spring-back deformation of cross ply is larger than uni-directional for the case of graphite and invar moulds, which is a consequence of a constrained transverse contraction of the laminate, strains due to the chemical shrinkage and a thermal contraction act predominately in thickness direction which explains an increased spring-back

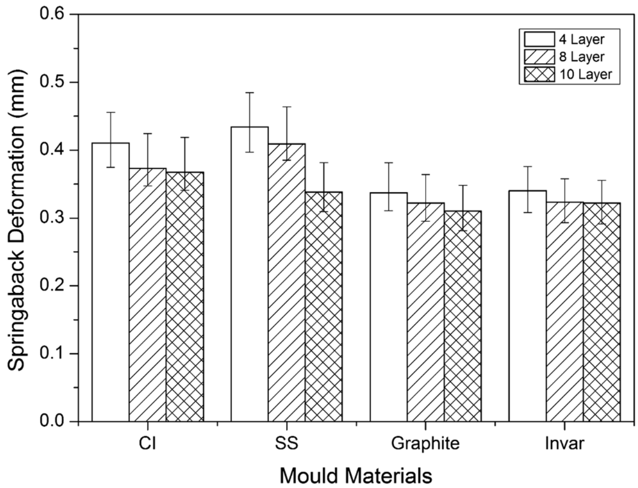

Fig. 12. Effect of number of layers on spring-back deformation.

deformation.

4.4. Effect of laminate thicknesses

The effect of laminate thickness has also been studied for three varying sample sizes of 0.8 mm, 1.6 mm and 2.0 mm having 4, 8 and 10 layers respectively. Total 24 experiments, six for each mould material have been conducted considering different curing cycles and lay-up sequences for each laminate thicknesses. It is evident from the Fig. 12 that thin components have greater spring-back deformation than corresponding thick components. Since, the area moment of inertia is $I \sim t^3$, a small deviation in a laminate thickness significantly affects the measured deflection. If data for each thickness has been normalised by spring-back of 4 plies parabolic laminate, then normalised averaged spring-back is best fitted with a $1/t^2$ curve rather than the $1/t$ and $1/t^3$ curves [5,34] and it supports the effect of a laminate thickness on spring-back deformation.

4.5. Interaction effect of process parameters

The previous subsections describe the effect of the individual parameter on spring-back deformation, whereas interaction plots allow the examination of all process parameters simultaneously to identify key parameters. Strong interaction effects are present for mould materials, laminate thickness and lay-up sequences, with medium interaction effects present for curing cycle as demonstrated in Fig. 13. From interaction plots, it can be clearly seen that among all combinations of process parameters with invar mould material, single hold curing cycle, quasi-isotropic lay-up sequence, 2 mm laminate thickness have a minimum spring-back deformation of 0.26 mm. Stainless steel mould material, double hold curing cycle, uni-directional lay-up sequence and 0.8 mm laminate thickness gives maximum spring-back deformation of 0.51 mm.

The interaction effects of all process parameters on the spring-back deformation have also been realised using the surface contour plots. Fig. 14 shows the surface plots for spring-back deformation prepared using response surface methodology for different mould materials. The overall spring-back deformation for double hold curing cycle is a little

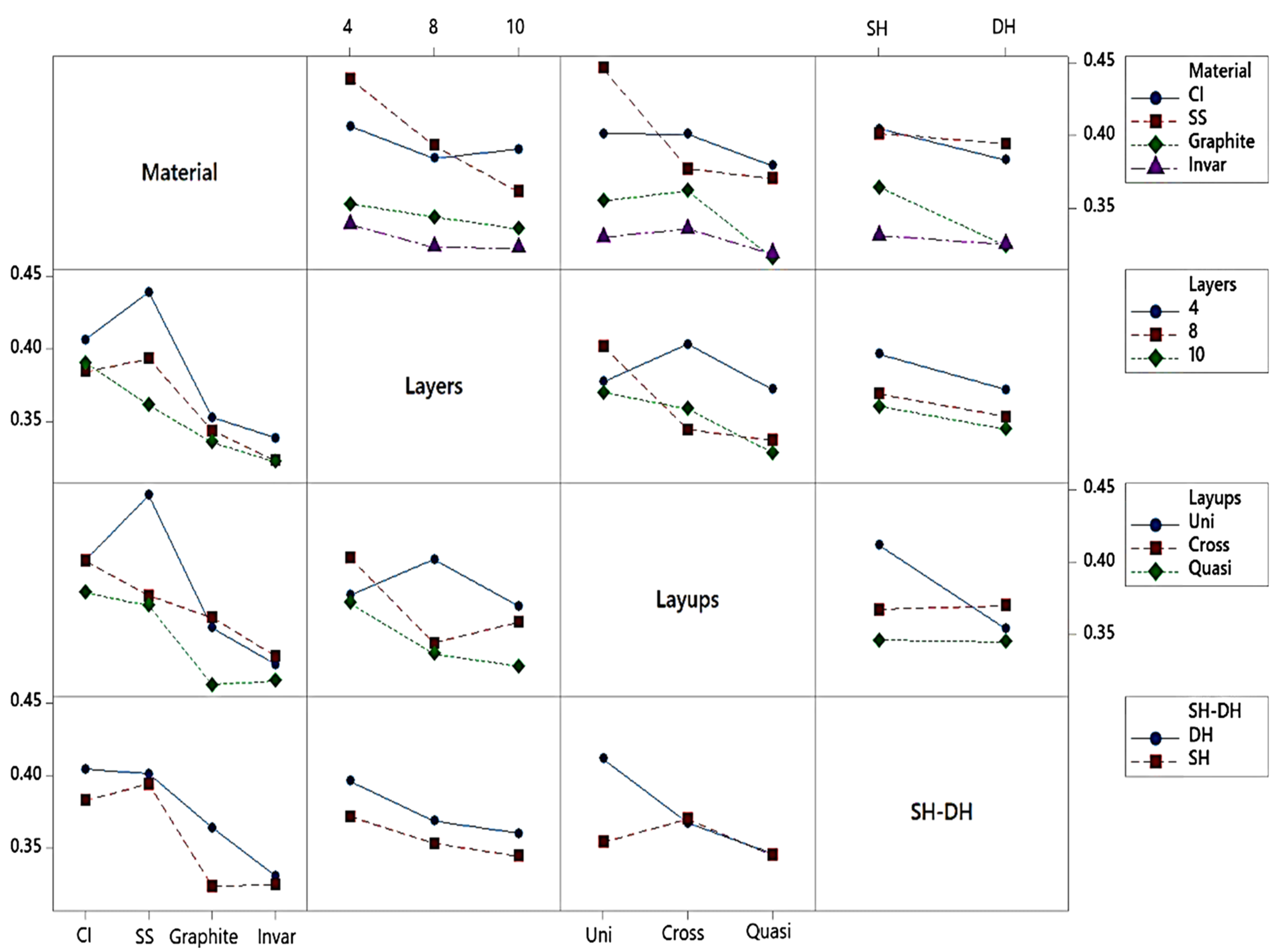

Fig. 13. Interaction plots for process parameters on spring-back deformation.

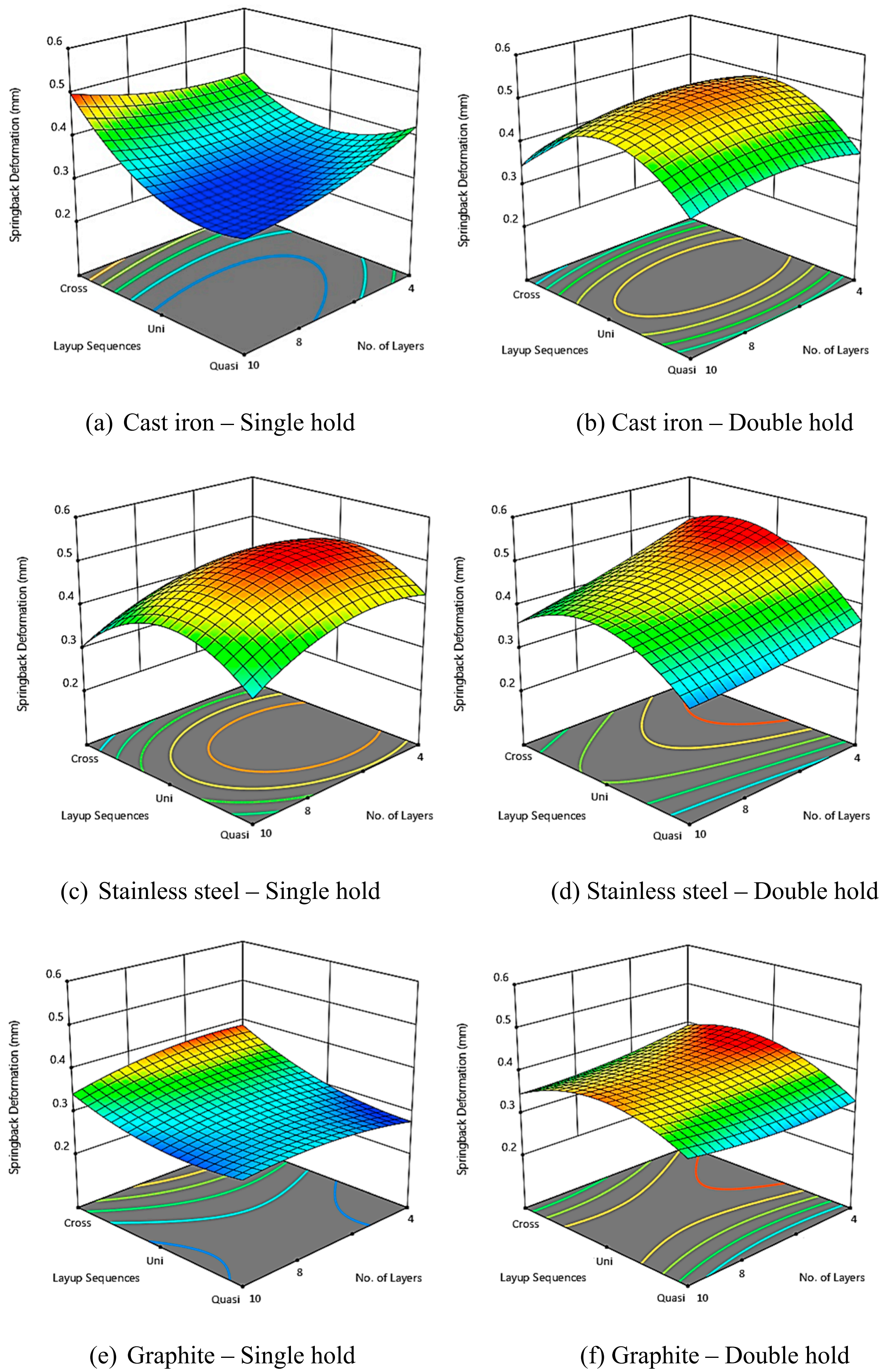

Fig. 14. Response surface graphs of spring-back deformation. (For interpretation of the references to colour in this figure legend, the reader is referred to the web version of this article.)

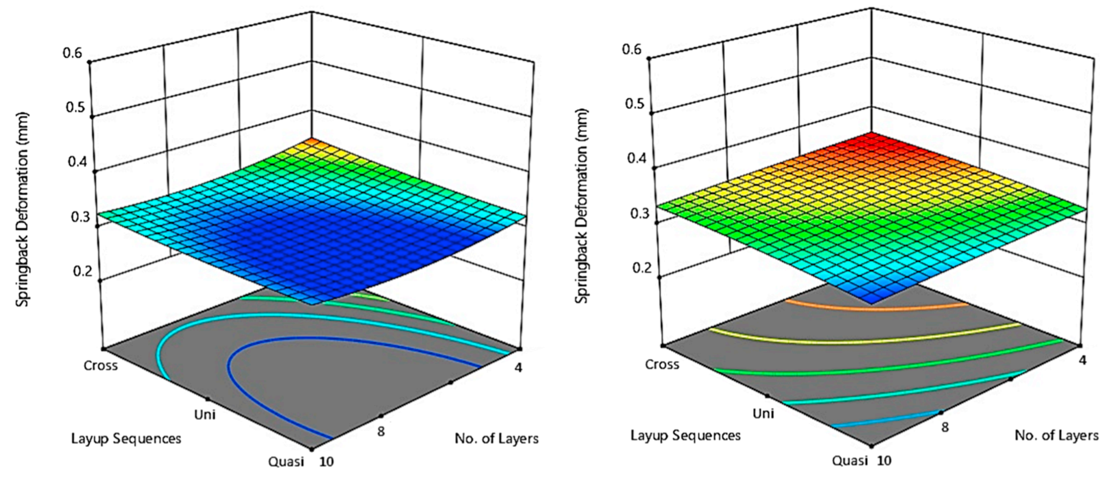

(g) Invar – Single hold (h) Invar – Double hold

Fig. 14. (*continued*)

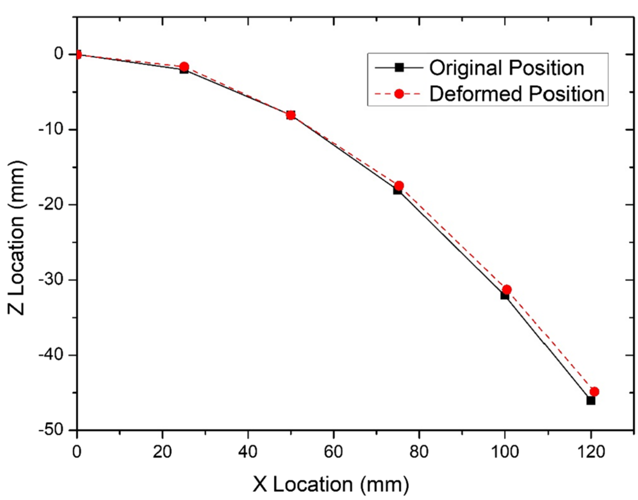

Fig. 15. Comparison of deformed and original position for parabolic reflector antenna (deformation scale factor = 10). (For interpretation of the references to colour in this figure legend, the reader is referred to the web version of this article.)

more compared to single hold curing cycle in each case of mould materials. The value for spring-back deformation is less than 0.4 mm in case of invar and graphite mould materials compared to cast iron and stainless steel mould materials with any combination of other process parameters. The spring-back deformation is minimum for 10 layers with quasi-isotropic lay-up sequence for each mould material with any curing cycle. The spring-back deformation is maximum for 4 layers with cross lay-up sequence for invar and graphite mould materials and with uni-directional lay-up sequence for stainless steel and cast iron mould materials.

The spring-back deformation of the stainless steel mould, quasi-isotropic lay-up sequence with 8 layers and double hold curing cycle has been plotted. The locations of 11 points along the central *X-Z* plane on the mould side of the reflector have been chronicled and plotted as shown in Fig. 15. The measured shape of this cross-section corresponds to shape of the 3D reflector at a location where the 2D cross-section has been determined by curve fitting of the scanned data points at that location. Due to symmetry about *Z*-axis, only one half of 2D cross-section has been shown in Fig. 15. The maximum measured spring-back has been observed at the outer periphery of the reflector.

To analyse the effect of spring-back deformation in $X-Y$ section, 40 coordinate points on the outer perimeter of the reflector have been selected. It is noted that the maximum spring-back deformation has been observed at the outer periphery of the reflectors. The maximum spring-back deformation has been obtained in the case of stainless steel mould with 4 layers and double hold curing cycle for different lay-up sequences. The said combinations have been selected for this analysis. The locations of 40 points along the $X-Y$ section on reflector have been chronicled and plotted as shown in Fig. 16(a). The deformed shape has also been plotted for uni-directional, cross and quasi-isotropic lay-up sequences. The measured elliptical shape has been compared with the original circular shape of the reflectors. The maximum ratio of long to the short axis for elliptical shape has been obtained as 1.0143, giving 1.4% difference to the original shape. The similar procedure has been followed for other mould materials and process parameters. The minimum spring-back deformation has been found for reflectors fabricated using invar mould material. The measured elliptical shape along with original circular shape for invar mould with 10 layers, single hold curing cycle and uni-directional, cross and quasi-isotropic lay-up sequences have been plotted as shown in Fig. 16(b). The minimum ratio of long to the short axis for elliptical shape has been obtained as 1.00528, giving 0.5% difference to the original shape.

5. Conclusion

The effect of process parameters on the spring-back deformation during an autoclave curing of parabolic antenna reflectors has been investigated experimentally. Total 72 antenna reflectors have been manufactured using the autoclave curing process with the combination of various process parameters. The parabolic shape moulds have been machined using grey cast iron 30, stainless steel AISI 430, graphite EDM and invar 36 on a 5-axis vertical machining centre with the identical surface finish. The carbon fiber prepreg layers along with consolidation materials have been laid on mould in proper sequence. Two different curing cycle – single hold and double hold have been applied to an autoclave machine for CFRP prepreg curing. The cured reflectors have been measured at 200 identical locations using high precision 3D scanning technique. The spring-back deformation has been determined based on the differences in RMS value for each coordinates points of CAD model and manufactured reflectors.

The mould materials and laminate thickness have a major effect on spring-back deformation because of mould part interaction and area moment of inertia respectively. The average spring-back deformation with invar mould material is almost 21% lesser than that with stainless

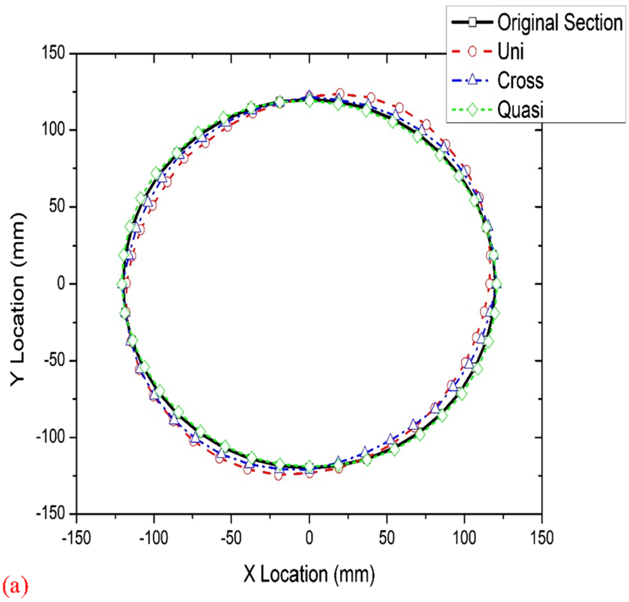

(a)

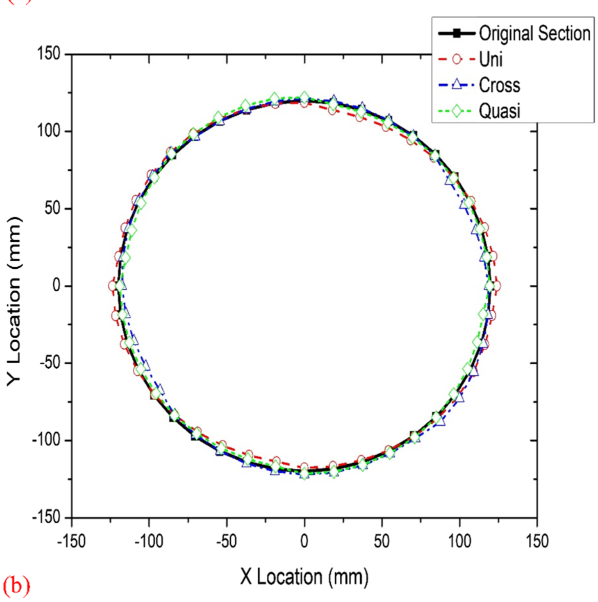

(b)

Fig. 16. Comparison of deformed and original $X-Y$ section for (a) steel mould, double hold curing cycle, 4 layers (b) invar mould, single hold curing cycles, 10 layers (deformation scale factor = 10). (For interpretation of the references to colour in this figure legend, the reader is referred to the web version of this article.)

steel mould material. The average spring-back deformation of 2 mm laminate thickness is nearly 12% lesser than 0.8 mm laminate thickness reflector. The effect of lay-up sequences for cast iron and stainless steel mould have medium effect whereas for graphite and invar mould as well as curing cycle has less effect on spring-back deformation of antenna reflectors. The average spring-back deformation for quasi-isotropic lay-up sequence is almost 10% lesser than uni-directional lay-up sequence and 6% lesser than cross lay-up sequence. The average spring-back deformation for single hold curing cycle is nearly 5% lesser than double hold curing cycle reflectors. The combination of invar mould material, single hold cycle, quasi-isotropic lay-up sequence and 2 mm laminate thickness has lowest spring-back deformation among all combinations. The reflector fabricated using stainless steel mould material, double hold curing cycle, uni-directional lay-up sequence and 0.8 mm laminate thickness has highest spring-back deformation.

Acknowledgements

The study was financially supported by Indian Space Research Organisation (ISRO), Department of Space, India for the Respond Project titled “Process development for minimization of spring-back deformation and enhancement for profile accuracy of CFRP reflectors.” wide letter No. ISRO/RES/3/671/14-15, Dated 18/03/2015. The authors would also like to acknowledge the experimental and a material characterisation support provided by Manipal University, Manipal, India and Ahmedabad Textile Industry’s Research Association (ATIRA), Ahmedabad, India respectively. M/s. KR Composites Pvt. Ltd., Surat, India and M/s. Vactech Composites Pvt. Ltd., Vapi, India are also acknowledged for providing the consolidation material free of cost.

References

[1] Kaw Autar K. Mechanics of composite materials CRC Press; 2006. https://doi.org/10.1016/j.fsigen.2011.07.001.
[2] Mazumdar SK. Composites manufacturing: materials, product, and process engineering. CRC Press; 2002.
[3] Hahn HT, Pagano NJ. Curing stresses in composite laminates. J Compos Mater 1975;9:91–106. https://doi.org/10.1177/002199837500900110.
[4] White SR, Hahn HT. Process modeling of composite materials: residual stress development during cure. Part I. model formulation. J Compos Mater 1992;26:2402–22. https://doi.org/10.1177/002199839202601604.
[5] Twigg G, Poursartip A, Fernlund G. Tool-part interaction in composites processing. Part I: Experimental investigation and analytical model. Compos Part A Appl Sci Manuf 2004;35:121–33. https://doi.org/10.1016/S1359-835X(03)00131-3.
[6] Twigg G, Poursartip A. Tool – part interaction in composites processing. Part II: numerical modelling. Compos Part A 2004;35:135–41. https://doi.org/10.1016/S1359-835X(03)00132-5.
[7] Kaushik V, Raghavan J. Experimental study of tool-part interaction during autoclave processing of thermoset polymer composite structures. Compos Part A Appl Sci Manuf 2010;41:1210–8. https://doi.org/10.1016/j.compositesa.2010.05.003.
[8] de Oliveira R, Lavanchy S, Chatton R, Costantini D, Michaud V, Salathé R, et al. Experimental investigation of the effect of the mould thermal expansion on the development of internal stresses during carbon fibre composite processing. Compos Part A Appl Sci Manuf 2008;39:1083–90. https://doi.org/10.1016/j.compositesa.2008.04.011.
[9] Stefaniak D, Kappel E, Spröwitz T, Hühne C. Experimental identification of process parameters inducing warpage of autoclave-processed CFRP parts. Compos Part A Appl Sci Manuf 2012;43:1081–91. https://doi.org/10.1016/j.compositesa.2012.02.013.
[10] Albert C, Fernlund G. Spring-in and warpage of angled composite laminates. Compos Sci Technol 2002;62:1895–912. https://doi.org/10.1016/S0266-3538(02)00105-7.
[11] Fernlund G, Poursartip A, Twigg G, Albert C. Residual stress, spring-in and warpage in autoclaved composite parts. 14th Int Conf Compos Mater; 2003.
[12] Huang CK, Yang SY. Warping in advanced composite tools with varying angles and radii. Compos Part A Appl Sci Manuf 1997;28:891–3. https://doi.org/10.1016/S1359-835X(97)00045-6.
[13] Dong C. Modeling the dimensional variations of composites using effective coefficients of thermal expansion. J Compos Mater 2009;43:2639–52. https://doi.org/10.1177/0021998309345296.
[14] Vargas G, Arrese a, Carbajal N, Mujika F. Analysis of in-plane and out-of-plane thermo-mechanical stresses in un-symmetric cross-ply curved laminated strips. J Compos Mater 2009;43:3157–84. https://doi.org/10.1177/0021998309345321.
[15] Yuan Z, Wang Y, Peng X, Wang J, Wei S. An analytical model on through-thickness stresses and warpage of composite laminates due to tool-part interaction. Compos Part B Eng 2016;91:408–13. https://doi.org/10.1016/j.compositesb.2016.01.016.
[16] Nelson RH, Cairns DS. Prediction of dimensional changes in composite laminates during cure. In: 34th Int SAMPE Symp; 1989. p. 2397–410.
[17] Bapanapalli SK, Smith LV. A linear finite element model to predict processing-induced distortion in FRP laminates. Compos Part A Appl Sci Manuf 2005;36:1666–74. https://doi.org/10.1016/j.compositesa.2005.03.018.
[18] Darrow D, Smith LV. Isolating components of processing induced warpage in laminated composites. J Compos Mater 2002;36:2407–19. https://doi.org/10.1106/002199802026784.
[19] Kappel E, Stefaniak D, Spröwitz T, Hühne C. A semi-analytical simulation strategy and its application to warpage of autoclave-processed CFRP parts. Compos Part A Appl Sci Manuf 2011;42:1985–94. https://doi.org/10.1016/j.compositesa.2011.09.001.
[20] Kappel E, Stefaniak D, Hühne C. Process distortions in prepreg manufacturing - An experimental study on CFRP L-profiles. Compos Struct 2013;106:716–23. https://doi.org/10.1016/j.compstruct.2013.07.020.
[21] Kappel E, Stefaniak D, Holzhüter D, Hühne C, Sinapius M. Manufacturing distortions of a CFRP box-structure - A semi-numerical prediction approach. Compos Part A Appl Sci Manuf 2013;51:89–98. https://doi.org/10.1016/j.compositesa.2013.04.003.
[22] Wisnom MR, Potter KD, Ersoy N. Shear-lag analysis of the effect of thickness on spring-in of curved composites. J Compos Mater 2006;41:1311–24. https://doi.org/

10.1177/0021998306068072.

[23] Kappel E. Spring-in of curved CFRP/foam-core sandwich structures. Compos Struct 2015;128:155–64. https://doi.org/10.1016/j.compstruct.2015.03.058.

[24] Marchetti M, Morganti F, Tizzi S. Evaluation of the built-in stresses and residual distortions on cured composites for space antenna reflectors applications. Compos Struct 1987;7:267–83. https://doi.org/10.1016/0263-8223(87)90079-1.

[25] Datashvili L, Nathrath N, Lang M, Baier H, Fasold D, Pellegrino S. New concepts and reflecting materials for space borne large deployable reflector antennas. In: 28th ESA Antenna Work Sp Antenna Syst Technol; 2005.

[26] Team P. GSAT-18 - preliminary design review document. Space Applications Centre, Indian Space Research Organisation (ISRO), Ahmedabad; 2016.

[27] Hinpreg ® A45 epoxy matrix - product data. Hindoostand Technical Fabrics; 2015.

[28] Fernlund G, Rahman N, Courdji R, Bresslauer M, Poursartip A, Willden K, et al. Experimental and numerical study of the effect of cure cycle, tool surface, geometry, and lay-up on the dimensional fidelity of autoclave-processed composite parts. Compos - Part A Appl Sci Manuf 2002;33:341–51. https://doi.org/10.1016/S1359-835X(01)00123-3.

[29] Jones RM. Mechanics of composite materials. Taylor & Francis Group, LLC 1999. https://doi.org/10.1007/BF00611782.

[30] Fernlund G, Osooly A, Poursartip A, Vaziri R, Courdji R, Nelson K, et al. Finite element based prediction of process-induced deformation of autoclaved composite structures using 2D process analysis and 3D structural analysis. Compos Struct 2003;62:223–34. https://doi.org/10.1016/S0263-8223(03)00117-X.

[31] Imbriale William, Steven Gao LB. Space antenna handbook. John Wiley & Sons; 2012.

[32] Fernlund G, Poursartip A. The effect of tooling material, cure cycle, and tool surface finish on spring-in of autoclave processed curved composite parts. ICCM 1999.

[33] Jain LK, Lutton BG, Mai Y-W, Paton R. Stresses and deformations induced during manufacturing. Part II: A study of the spring-in phenomenon. J Compos Mater 1997;31:696–719. https://doi.org/10.1177/002199839703100704.

[34] Mezeix L, Seman A, Nasir MNM, Aminanda Y, Rivai A, Castanié B, et al. Spring-back simulation of unidirectional carbon/epoxy flat laminate composite manufactured through autoclave process. Compos Struct 2015;124:196–205. https://doi.org/10.1016/j.compstruct.2015.01.005.